Structure of the First Transmembrane Domain of the Neuronal Acetylcholine Receptor β_2 Subunit

Vasyl Bondarenko,* Yan Xu,*† and Pei Tang*†‡
Departments of *Anesthesiology, †Pharmacology, and ‡Computational Biology, University of Pittsburgh School of Medicine, Pittsburgh, Pennsylvania 15260

ABSTRACT The recent cryoelectron microscopy structure of the *Torpedo* nicotinic acetylcholine receptor (nAChR) at 4-Å resolution shows long helices for all transmembrane (TM) domains. This is in disagreement with several previous reports that the first TM domain of nAChR and other Cys-loop receptors are not entirely helical. In this study, we determined the structure and backbone dynamics of an extended segment encompassing the first TM domain (TM1e) of nAChR β_2 subunit in dodecylphosphocholine micelles, using solution-state NMR and circular dichroism (CD) spectroscopy. Both CD and NMR results show less helicity in TM1e than in *Torpedo* nAChR structure (Protein Data Bank: 2BG9). The helical ending residues at the C-terminus are the same in the TM1e NMR structure and the *Torpedo* nAChR structure, but the helical starting residue (I-217) in TM1e is seven residues closer to the C-terminus. Interestingly, the helical starting residue is two residues before the highly conserved P-219, in accordance with the hypothesis that proline causes helical distortions at three residues preceding it. The NMR relaxation measurements show a dynamics pattern consistent with TM1e structure. The substantial nonhelical content adds greater flexibilities to TM1e, thereby implicating a different molecular basis for nAChR function compared to a longer and more rigid helical TM1.

INTRODUCTION

Receptors of the Cys-loop superfamily, including γ-amino-butyric acid type A, glycine, serotonin, and acetylcholine receptors, are responsible for fast synaptic transmission in the central and peripheral nervous systems. They are either homo- or heteropentameric ion channels that can be activated by the binding of neurotransmitters. Each receptor is composed of five subunits and each subunit has an extended extracellular N-terminal domain, four transmembrane (TM) domains (TM1–TM4) with the TM2 lining the channel, and a short C-terminus (1–3). A significant conformation change of receptors is anticipated during the channel activation. The current structural understanding of the Cys-loop receptors is largely based on the structure data acquired on the nicotinic acetylcholine receptor (nAChR) and the acetylcholine-binding proteins (AChBP), a soluble homolog of the amino-terminal domain of a Cys-loop receptor. The high-resolution x-ray structures of AChBP in ligand-free and ligand-bound states provide atomic details of ligand binding sites of Cys-loop receptors (4,5). The structure model from cryoelectron microscopy (cryo-EM) of the *Torpedo* nAChR at a resolution of 4 Å offers the first glimpse of a Cys-loop receptor and reveals the spatial relationship between the extracellular binding domain and TM channel domain (6), allowing us to perceive the functional couplings between different regions of the receptors.

A striking feature of the cryo-EM *Torpedo* nAChR structure (6) is its extremely high helicity in the four TM domains. Although the helical structure of TM domains has been suggested by many experiments, it remains controversial as to whether every TM segment is a linear α-helix (7–9). Among all TM domains, TM1 appears to be most susceptible to possessing a substantial amount of nonhelical elements (10–19). Because TM1 is the only TM segment that links covalently to the ligand-binding domain, it can potentially play an important role in the regulation of channel functions. Using the substituted cysteine accessibility method (20), it was concluded that the N-terminal third of TM1 contributes to the lining of the channel and undergoes conformational change during gating. Mutations at the conserved proline residue of TM1 (Pro-219 in the original β_2 sequence, Pro-14 in TM1e) lead to receptors that require abnormally high concentration of agonists to gate (21). Other mutation studies also suggested the involvement of TM1 in nAChR function (22–25). If a considerable nonhelical structure component is indeed present in the TM1 domain, it can render certain flexibility to fulfill the requirement of conformation changes during the process of channel gating. Therefore, a precise TM1 structure with atomic resolution is vital to gaining insight into the channel function.

It has been elegantly demonstrated by sampling a large database that proline residues can introduce a region of flexibility in the TM structure because of steric hindrance and the loss of hydrogen bonds, and the location of the hinges is about one turn of helix (3 or 4 residues) N-terminal to the proline residues (26). Residue Pro-14 in the center segment of TM1e is conserved in all Cys-loop receptors and may cause distortions in the normal helical structure. In this study, we

Submitted August 15, 2006, and accepted for publication November 13, 2006.

Address reprint requests to Professor Pei Tang, PhD, 2049 Biomedical Science Tower 3, 3501 Fifth Ave., University of Pittsburgh, Pittsburgh, PA 15260. Tel.: 412-383-9798; Fax: 412-648-8998; E-mail: tangp@anes.upmc.edu.

0006-3495/07/03/1616/07 $2.00

doi: 10.1529/biophysj.106.095364

determined the structure and backbone dynamics of the TM1 of the human nAChR β_2-subunit using solution-state NMR and circular dichroism (CD) spectroscopy. At atomic resolution, the NMR structure of TM1e exhibits less helical content than the cryo-EM structure model of the *Torpedo* nAChR (6,27). The nonhelical location induced by proline is in line with the empirical prediction (26). The substantial nonhelical structure adds great flexibilities to TM1, thereby implicating a different molecular basis for channel function compared to the scenario of a longer and more rigid TM1 helix.

MATERIALS AND METHODS

Sample preparation

TM1 of nAChR includes only 20 amino acids according to the conventional definition from the hydropathy plot (27). To prevent truncation-induced structure distortion, we included an additional 10 and 5 residues from the N- and C-termini of TM1, respectively, in the segment for our study. This extended TM1 segment with 35 amino acid residues is designated as TM1e. TM1e of the human neuronal nAChR β_2 subunit was obtained by solid-phase synthesis using the same protocol as described previously (28). The sequence and residue numbering of TM1e are given in Table 1, and residues Leu, Phe, Ile, Ala, and Val are ^{15}N labeled. For preparing the NMR and CD samples, TM1e was first dissolved in trifluoroethanol and dried into a thin film under a stream of nitrogen gas. An aqueous solution of perdeuterated dodecylphosphocholine (DPC)-d_{38} was then added to reach a DPC/peptide molar ratio of 150. After being vigorously mixed, the sample was lyophilized and rehydrated with 10% D_2O and 90% H_2O to a final peptide and DPC concentration of 0.83 and 125 mM, respectively. D_2O was required for deuterium lock in the NMR measurements. DPC-d_{38} and D_2O were obtained from Cambridge Isotope Laboratories (Andover, MA).

CD spectroscopy

CD spectra were acquired at 25°C in the wavelength range of 190–290 nm on an Aviv CD spectrometer (model 202, Aviv Instruments, Lakewood, NJ) with a 1-mm cuvette. After solvent subtraction, the spectra were analyzed using the web-based CD analysis software DICHROWEB at www.cryst.bbk.ac.uk/cdweb/html/home.html (29).

NMR spectroscopy

NMR spectra were collected at 30°C on two Bruker Avance-600 NMR spectrometers equipped with a triple-resonance inverse TXI probe and a triple-resonance inverse, TCI, cryoprobe. A series of NMR experiments was performed for the chemical shift assignment and structure determination of TM1e. ^{15}N-decoupled ^{1}H homonuclear nuclear Overhauser effect spectroscopy (NOESY) and total correlation spectroscopy (TOCSY) spectra were acquired with 2048 × 512 data points and a spectral width of 12 ppm in each dimension. The mixing times for NOESY and TOCSY were 100–150 ms and 60 ms, respectively. All spectra were obtained in the phase-sensitive mode with a relaxation delay of 1.2 s. The WATERGATE pulse scheme was applied for solvent suppression. Gradient-selected, sensitivity-enhanced ^{1}H-^{15}N heteronuclear single-quantum correlation (HSQC) spectra were collected as 2048 × 80 data points, with a spectral width of 15 ppm for both ^{1}H and ^{15}N dimensions. HSQC spectra were acquired at five different temperatures, ranging from 20°C to 40°C, for evaluating temperature dependence of chemical shifts of individual residues. The residues with temperature coefficients <0.004 ppm/K are considered to have hydrogen bonding (30). Three-dimensional (3D) NOESY-HSQC data were collected with a mixing time of 100 ms, a relaxation delay of 1 s, and 2048 × 128 × 48 data points. The observed ^{1}H chemical shifts were referenced to the 2,2-dimethyl-2-silapentene-5-sulfonate resonance at 0 ppm, and the ^{15}N chemical shifts were indirectly referenced (31). To characterize the dynamic property of TM1e, spin-lattice (R_1) and spin-spin (R_2) ^{15}N relaxation rate constants and ^{15}N-{^{1}H} heteronuclear Overhauser effects (NOE) were measured repeatedly for each of the ^{15}N amides using standard pulse sequences with Echo-Antiecho gradient selection (32). Each spectrum has 2048 × 80 data points and a spectral width of 15 ppm for both ^{1}H and ^{15}N dimensions. The R_1 spectra were acquired with a fixed interval of 2.3 s between scans and nine variable delays ranging from 10 to 2290 ms. Ten variable delays in the range of 16 and 160 ms and a recycle delay of 1.8 s were used for the R_2 measurement. In NOE experiments, the saturation was achieved by a train of 120° pulses at 5 ms intervals for 3 s.

Data process and analysis

All NMR data were processed using NMRPipe 4.1 and NMRDraw 1.8 (33) and analyzed using SPARKY 3.110 (34) programs. Structures were calculated using XPLOR-NIH (35), and their quality was checked using PROCHECK (36). Distance restraints derived from two-dimensional (2D) NOESY and 3D NOESY-HSQC data were grouped into four categories: 1.8–2.7, 1.8–3.3, 1.8–5.0, and 1.8–6.0 Å for strong, medium, weak, and very weak NOEs, respectively (37). The initial structural calculations were carried out using only the NOE restraints with the simulated annealing protocol (38) in XPLOR-NIH (35,39). Sixty lowest energy structures with no violations above the threshold conditions, which are 5° for all angles, 0.05 Å for bonds, and 0.5 Å for NOEs, were taken for further refinement. The hydrogen-bond restraints of the backbone [i.e., CO(i) to NH(i + 4)] were included in the refinement if the $d_{\alpha N}(i,i+3)$ or $d_{\alpha\beta}(i,i+3)$ NOE connectivity was present. Each hydrogen bond was converted into two distance restraints: $r_{NH\text{-}O}$ (1.2–1.9 Å) and $r_{N\text{-}O}$ (1.8–2.9 Å) (40,41). Visualization and analysis of the protein structures including root mean-squared deviation (RMSD) calculation were carried out using the MOLMOL (42) and VMD (43) programs. In dynamics studies, R_1 and R_2 values of backbone ^{15}N were determined from two-parameter, single-exponential fitting of the peak intensities versus the variable delays. ^{15}N-{^{1}H} NOE values were calculated as peak intensity ratios obtained with and without ^{1}H saturation. The global tumbling time (τ_m) of TM1e in DPC micelles was initially estimated from the R_2/R_1 ratio (44). The squared order parameter (S^2), the exchange rate constant (R_{ex}), the effective correlation time for fast internal motions (τ_e), and the refined τ_m value were obtained by fitting the experimentally measured R_1, R_2, and NOE values in the framework of Lipari-Szabo Model free formalism (45,46) and subsequent Monte Carlo numerical simulations using Tensor 2 (47).

RESULTS

The α-helical content of TM1e in DPC micelles was evaluated using CD spectroscopy. The CD spectrum of TM1e in

TABLE 1 The amino acid sequence of the TM1e domain of the human *n*-acetylcholine receptor β_2 subunit

Sequence numbering	210	215	220	225	230	235	240
Relative numbering	5	10	15	20	25	30	35
nAChR-β_2	RRKPL	FYTIN	LIIPC	VLITS	LAILV	FYLPS	DCGEK

The original sequence numbering and the relative numbering used in this study are given in the first and second rows, respectively. The underlined residues are ^{15}N-labeled.

Fig. 1 was analyzed by the CDSSTR method in the web-based DICHROWEB package (29) and reveals 49% of the α-helical content that corresponds to 17 residues.

NMR experiments provided more detailed structural information of TM1e. The chemical shift assignment of TM1e was achieved by TOCSY and NOESY experiments. The HSQC spectrum of TM1e in Fig. 2 shows 16 well-resolved crosspeaks from all ^{15}N-labeled residues. A significant reduced peak intensity of residue Leu-11, three residues apart from Pro-14, is noticeable.

Fig. 3 summarizes the structural information of TM1e obtained from 2D and 3D NOESY spectra. The midrange NOE connectivity (H^{α}_{i}-H^{N}_{i+3}, H^{α}_{i}-H^{β}_{i+3}, and H^{α}_{i}-H^{N}_{i+4}) was found from Ile-12 to Tyr-27, indicating a helical structure in this region. The chemical shift index (CSI), determined on the basis of H^{α} proton chemical shifts from the corresponding random coil values (48), also implies a helix between Ile-12 and Phe-26. Hence, the helicity of TM1e delineated from NMR (15 residues) is in good agreement with the CD result (16–17 residues). It is noteworthy that the low intensity of residue Leu-11 in Fig. 2 might result from the residue's special location. Leu-11 is at a hinge point where the CSI changes the sign and the midrange NOE connectivity begins to appear in Fig. 3. Several residues at the N-terminus of TM1e, from residues Pro-4 to Leu-11, are predicted to be in the TM helix based on the hydrophobicity scale (49) and appear to be in the helix in the *Torpedo* structure model (6,27) but show no sign of helicity in any of our NMR measurements. The absence of the helical structure from Leu-28 to Leu-35 in the NMR results, however, is in accord with the hydrophobicity prediction and the *Torpedo* structure model (6,27).

The statistics of a bundle of the 20 lowest energy NMR structures is listed in Table 2. The helical region between Ile-12 and Phe-26 has a small RMSD of 0.10 ± 0.03 Å for the backbone and 0.85 ± 0.15 Å for all heavy atoms. It is clearly demonstrated in Fig. 4, *A* and *B*, that a typical NMR structure of TM1e is at least one helical turn less than the corresponding region of the *Torpedo* structure from the cryo-EM data (6,27). Fig. 4 also shows that the hinge of helicity in the NMR structure is located at Leu-11, three residues N-terminal to Pro-14, indicating that Pro-14 acts in the same way as many TM proline residues, having the ability to disrupt α-helical structures (26).

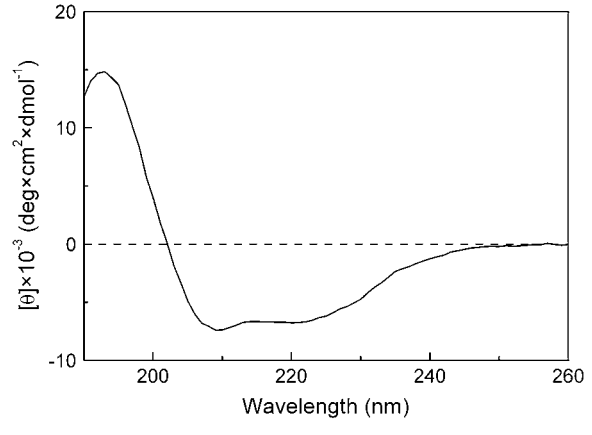

FIGURE 1 Far-ultraviolet CD spectrum of TM1e of the human *n*-acetylcholine receptor β_2 subunit in DPC micelles, showing ~49% helical content.

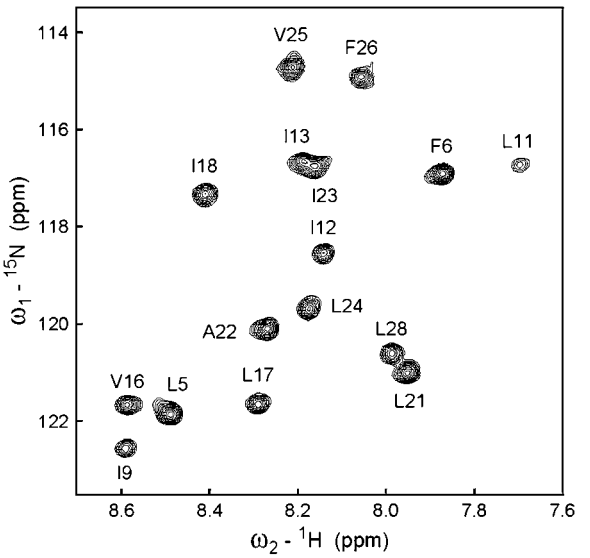

FIGURE 2 The backbone amide proton region of a ^{1}H-^{15}N HSQC NMR spectrum of 0.83 mM TM1e of the human *n*-acetylcholine receptor β_2 subunit in aqueous DPC micelles at 30°C. The resonance assignments are indicated by the one-letter amino acid code and the relative sequence number.

The dynamics properties of TM1e were determined by NMR relaxation measurements. ^{15}N R_1 and R_2 relaxation rates as well as ^{15}N-{^{1}H} NOE values of the ^{15}N-labeled

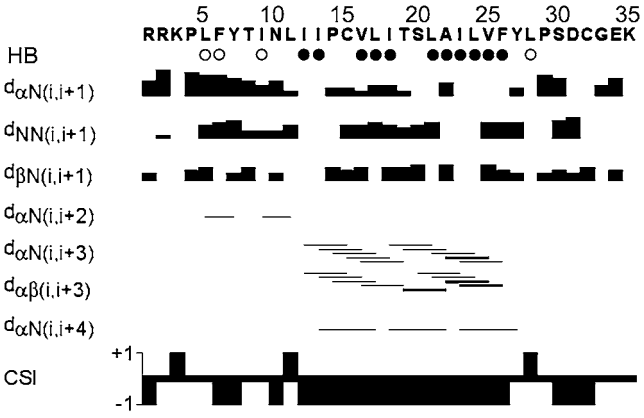

FIGURE 3 Summary of hydrogen-binding (HB) restraints, NOE connectivity, and the CSI for H^{α} protons of TM1e of the human *n*-acetylcholine receptor β2 subunit in DPC micelles. The residues, which temperature coefficients were smaller than 0.004 ppm/K, were considered being involved in HB (●). Otherwise, the residues were considered without HB (○). The temperature coefficient of Leu-11 was not determined due to its weak NMR signal. The remaining residues were not ^{15}N labeled, and their temperature coefficients were not determined. Sequential and midrange-range NOE connectivity is linked by line segments with widths proportional to the observed NOE intensities.

TABLE 2 Statistics for the family of the 20 lowest energy calculated structures of the TM1e peptide of the human *n*-acetylcholine receptor β_2 subunit

Distance restraints	
Intraresidue ($\mid i-j \mid = 0$)	80
Sequential ($\mid i-j \mid = 1$)	77
Medium-range ($2 < \mid i-j \mid \leq 4$)	34
Number of NOEs per residue	5.5
Number of H-bond restraints (two per bond)	22
Total numbers of restraints	213
Number of refined structures	20
Energy (kcal/mol)	
E_{NOE}*	15.5 ± 3.4
E_{dihe}*	80.9 ± 12.9
E_{impr}	5.5 ± 0.7
E_{ele}	−244.7 ± 30.3
RMSD (Å)	
Residue numbers	12–26
Backbone	0.10 ± 0.03
Heavy atoms	0.85 ± 0.15
Ramachandran analysis (%)†	
Residues in favored region	73.1
Residues in additional allowed regions	22.9
Residues in generously allowed regions	4.0
Residues in disallowed regions	0.0

None of the structures has distance violations of >0.5 Å and dihedral angle violations of >5°.

*The final values of square-well NOE and dihedral angle potentials were calculated with force constants of 50 kcal mol^{-1} Å^{-2} and 200 kcal mol^{-1} rad^{-2}, respectively.

†Ramachandran analysis was performed using PROCHECK_NMR (35).

residues are shown in Fig. 5. The data for residue Leu-11 are omitted because of the potential errors resulting from the low NMR signal intensity of Leu-11. The patterns of R_1, R_2, and NOE changes along the TM1e sequence coincide well with the uncovered structure of TM1e. The nonhelix residues in the N- and C-termini have relatively higher R_1 and lower R_2 and NOE values, whereas the residues in the helical region have an opposite trend. The global tumbling time, τ_m, was estimated to be 14.2 ± 0.2 ns on the basis of the R_2/R_1 ratios of residues in the helical region (50). The τ_m value of 11.5 ns was derived later by further analysis of the NMR relaxation data using program Tensor 2 (47). The relaxation data analysis using Tensor 2 also yielded the square order parameter S^2, as shown in Fig. 5 *D*. The helical residues have S^2 in the range of 0.78–0.99, indicating restricted internal motions. In contrast, most of nonhelical residues show S^2 in the range of 0.49–0.60. Ile-9 is the only exceptional nonhelical residue that has an order parameter value compatible to those of the helical residues.

DISCUSSION

The recent *Torpedo* nAChR structure model derived from the 4-Å cryo-EM data disagrees with several previous experimental results in terms of helical content in the TM1 domain. The cryo-EM structure shows an exceptionally long

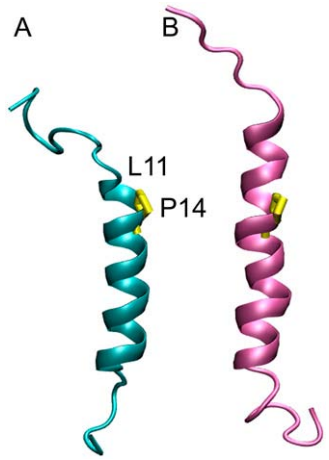

FIGURE 4 (*A*) One of the lowest energy NMR structures of TM1e and (*B*) the structure of the TM1 domain of the *Torpedo* nAChR β_1-subunit derived from the cryo-EM data (6) are shown for comparison. The highly conserved proline residue (Pro-14 in TM1e and Pro-227 in the β_1 subunits) is highlighted in yellow. Notice that the TM1e structure of the β_2 subunit has 15 residues in the helical region, compared to 20 residues in the structural model of the β_1 subunit derived from the 4-Å cryo-EM data.

helix consisting of ~29 residues in the α subunit (6) and 22 residues in the β subunit (6,27). Both CD and NMR data in our study indicate that the helical content in β_2 TM1e is significantly lower (15–17 residues). Low TM1 helicity was also suggested previously by others for the α-subunit of *Torpedo* nAChR. CD and Fourier transform infrared spectroscopy (FTIR) spectroscopy (13) of one or multiple

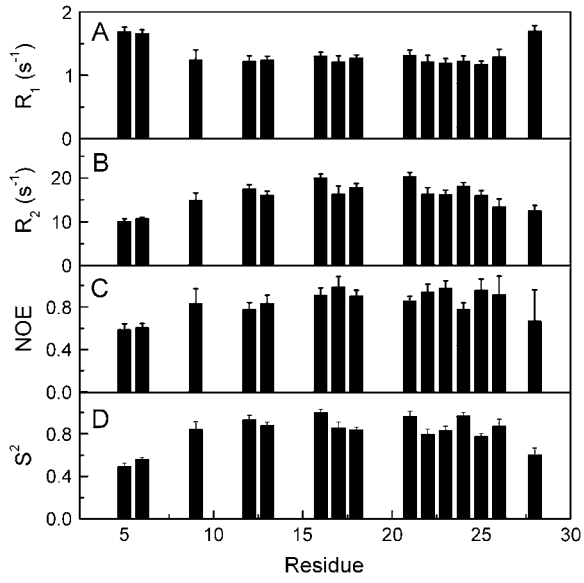

FIGURE 5 The longitudinal and transverse relaxation rate constants, (*A*) R_1 and (*B*) R_2, (*C*) the ^{15}N-{^{1}H} NOE values, and (*D*) the squared order parameter S^2 derived from the Tensor 2 analysis of the backbone amide ^{15}N of TM1e in DPC micelles at 30°C. Errors were derived from the uncertainties of the least-squares fitting to the exponential decay function (for R_1 and R_2) or from the signal/noise ratios (for NOE). For S^2, error bars are standard deviation derived from 300 Monte Carlo simulations.

TM domains from proteolytically digested AChR showed that TM1 in lipid (asolectin) has only 56% (~18 residues) α-helix, 15% β-turn, and as high as 29% ''other'' structural components. A substantial amount of nonhelical structure in TM1 was found in a fluorescence study of both the intact *Torpedo californica* nAChR and the TM peptides (15). Using combined fluorescence quenching and electron paramagnetic resonance collision gradient methods, it was concluded that the TM1 of the *T. californica* nAChR might form an irregular structure and span the membrane in a way different from a linear α-helix (14). Although the evolutionarily conserved proline residues was suspected of causing the irregular TM1 structure, none of these studies could provide direct evidence to support the hypothesis. Solid-state NMR on a selectively isotope-labeled TM1 segment of *T. californica* nAChR α-subunit in lipids (19) demonstrated that the deviations from helical conformation at the labeled residues αLeu-212, αIle-219, and αLeu-223 (homologs of Leu-5, Ile-12, and Val-16 in our case, respectively) could be as large as 50% if the sample was hydrated properly. Both αIle-219 and αLeu-223 are adjacent to the conserved proline. Because more residues are isotopically labeled in our TM1e and much better signal resolution can be achieved with solution NMR, we were able not only to directly observe the nonhelicity in TM1e, but also to provide more specific structural details, as depicted in Fig. 4. The N-terminus of TM1e is about one helical turn shorter than that proposed in the cryo-EM structure (6). The helix has 3.6 residues per turn, and each amino acid has a translation of 1.5 Å along the helical axis. The length of one helical turn (5.4 Å) is at the resolution limit where modeling of helices to match the electron (EM) density map is largely subjected to interpretation (for example, at the Fourier shell correlation coefficient of 0.6, none of the EM structure families had a resolution better than 5.5 Å. See supplementary materials of Unwin (6) and Miyazawa et al. (27). This resolution restraint may limit the accuracy of structural details. It was also suggested previously that the nonhelicity in TM1 increased with the rising sample hydration level (19). Hence, it is plausible that the TM1e structure determined by our solution-state NMR experiments reflects a more flexible TM1 conformation, whereas the EM structure (6) represents a different, more rigid conformation.

The frequent occurrence of the proline residue in the putative TM helices of integral membrane proteins, particularly transport proteins, is well recognized (51). However, among four TM domains of nAChR and other Cys-loop receptors, Pro-14 of TM1e is the only conserved proline residue in all Cys-loop receptors. The location of this conserved proline may not be an accident of the evolution. In accord with the empirical prediction (26), the identified hinge residue (Leu-11) of TM1e helix is three residues apart from the conserved Pro-14, indicating that the abruption of the helical structure in the N-terminal region of TM1e is indeed associated with the presence of Pro-14. As shown in Fig. 5, the nonhelical N-terminus of TM1e has smaller square order parameters, indicative of a much greater flexibility in the region. Such flexibility, imparted by the proline residue, might be a prerequisite for ligand-mediated modulation of nAChR function. The ligand binding in the extracelleular domain of the nAChR triggers the channel gating that is accompanied by the subsequent changes in ion current. The N-terminal TM1 is the only part in the TM domain that covalently links to the ligand-binding domain. Direct involvement of TM1 in the conformation change of nAChR has been suggested by several lines of experimental evidence (20–25). It seems plausible that a nonhelical structure at N-terminus of TM1 might better accommodate the required conformational change during the gating process. In other words, the flexibility of the TM1 domain to adopt different conformations is required as part of the transport cycle. A high-resolution structure of intact nAChR is necessary for further validation of the hypothesis.

In this study, TM1e structure and its dynamics were determined in DPC micelles. One might wonder how closely our results reflect the TM1 structure and dynamics of an intact nAChR. Ideally, one wants to solve the high-resolution structure of nAChR in one piece in the native lipid environment and at the physiologically relevant temperature. The feasibility to meet all these criteria is often inhibited by technique difficulties. Virtually no high-resolution structure is currently available for an intact nAChR. The cryo-EM structure (6), though missing several regions and having no side-chain information, nevertheless provides the basis for other complementary high-resolution studies, including the domain-by-domain approach by high-resolution NMR (28,52–54). The validity of such an approach has been tested recently by comparison of NMR structures of isolated segments of bacteriorhodopsin and lactose permease of *Escherichia coli* (lac Y) to the known x-ray structures of these membrane proteins (55,56). Small RMSD values of superimposed NMR and x-ray structures suggested that complementary high-resolution structural information could be achieved reliably via NMR studies of truncated domains. In fact, the application of the ''divide-and-conquer'' approach has been used for many high-molecular-weight proteins to avoid problems associated with spectral overlapping and line broadening in high-resolution NMR studies (57). In this context, individual domain structures have been found particularly useful as they provided an important foundation for further investigation of a larger complex or even an intact receptor protein. There is no particular reason to exclude nAChR from this approach. The previous fluorescence study already found the same topological pattern for reconstituted intact nAChR and derived TM peptides, thus validating the inferences made on the intact receptor topology using the studies with the isolated domains (15).

The structural discrepancy at the N-terminus between our TM1e and the homologs TM1 of *Torpedo* nAChR (6) naturally raises the question as to whether the low helical

content in TM1e truly reflects the secondary structure of the corresponding region in situ or simply results from some artifacts. Micelles are widely used in high-resolution solution-state NMR to mimic the membrane environment. Could the micelles introduce nonhelical structure in TM1e? As discussed above, the TM1 helicity of *Torpedo* nAChR α-subunit measured in lipid vesicles by CD and FTIR (13) was also much lower than that presented in the cryo-EM structure model (6). The length of the DPC carbon chain is unlikely to be the determinant of the low TM1e helicity. The diameter of a DPC micelle is ~46 Å on the basis of the apparent volume of a DPC micelle (58), whereas the determined helical length of TM1e is only ~21 Å. Longer TM helices have actually been previously determined in DPC micelles using solution-state NMR, such as a 19-residue helix in the TM2e of a human nAChR β_2 subunit (53) and a 21-residue helix in the TM2 of *N*-methyl D-aspartate (NMDA) receptor (52). Hence, micelles are unlikely to cause TM1e structural distortion. A possible source of artifacts is the sequence truncation at both ends of the segment, which could inevitably affect the terminal structure. However, the truncation usually affects much fewer residues than is found in the N-terminus of TM1e. As evidenced in our previous NMR study on TM2 of nAChR β_2-subunit in DPC micelles, the helix structure of TM2 started at the fourth residue (Thr) from the N-terminus (53). Besides, we have purposely extended TM1e by several residues into the presumed loop regions to avoid the truncation artifact. A few TM residues departing from the helical structure due to sequence truncation is expected, but it is hard to conclude that truncation could affect as many as 11 N-terminal residues in TM1e. Therefore, we tend to believe that at least part of the nonhelical structure at the TM1e N-terminus comes from the intrinsic property of TM1e rather than an artifact.

In conclusion, we have characterized the high-resolution structure and dynamics of the first TM domain of the β_2 subtype nAChR in DPC micelles using solution-state NMR. Our data not only support the previous finding that the TM1 structure of nAChR is not entirely helical (13,15,19) but also offer atomic details of helical and nonhelical regions. The overall helical content (15–17 residues) determined in this study is lower than that in the recent cryo-EM structure (6). The nonhelical N-terminal region of TM1e stops at Leu-11, which is three residues apart from the highly conserved proline residue (Pro-14), providing an additional line of evidence that the proline residue in the TM domain promotes a nonhelical structure. The nonhelical region of TM1e shows higher motion flexibility than the α-helix region. The higher flexibility in the N-terminus of TM1e may be necessary for the modulation of nAChR function.

SUPPLEMENTARY MATERIAL

An online supplement to this article can be found by visiting BJ Online at http://www.biophysj.org.

The authors thank Dr. Victor E. Yushmanov for the initial CD and NMR data acquisition and processing.

This work was supported in part by grants from the National Institutes of Health (R01GM56257 and R01GM66358 to P.T., and R37GM049202 and R01GM069766 to Y.X.).

REFERENCES

1. Karlin, A. 2002. Emerging structure of the nicotinic acetylcholine receptors. *Nat. Rev. Neurosci.* 3:102–114.
2. Lester, H. A., M. I. Dibas, D. S. Dahan, J. F. Leite, and D. A. Dougherty. 2004. Cys-loop receptors: new twists and turns. *Trends Neurosci.* 27:329–336.
3. Sine, S. M., and A. G. Engel. 2006. Recent advances in Cys-loop receptor structure and function. *Nature*. 440:448–455.
4. Brejc, K., W. J. van Dijk, R. V. Klaassen, M. Schuurmans, J. van Der Oost, A. B. Smit, and T. K. Sixma. 2001. Crystal structure of an ACh-binding protein reveals the ligand-binding domain of nicotinic receptors. *Nature*. 411:269–276.
5. Hansen, S. B., G. Sulzenbacher, T. Huxford, P. Marchot, P. Taylor, and Y. Bourne. 2005. Structures of Aplysia AChBP complexes with nicotinic agonists and antagonists reveal distinctive binding interfaces and conformations. *EMBO J.* 24:3635–3646.
6. Unwin, N. 2005. Refined structure of the nicotinic acetylcholine receptor at 4 Å resolution. *J. Mol. Biol.* 346:967–989.
7. Karlin, A., and M. H. Akabas. 1998. Substituted-cysteine accessibility method. *Methods Enzymol.* 293:123–145.
8. Cascio, M. 2004. Structure and function of the glycine receptor and related nicotinicoid receptors. *J. Biol. Chem.* 279:19383–19386.
9. Gorne-Tschelnokow, U., A. Strecker, C. Kaduk, D. Naumann, and F. Hucho. 1994. The transmembrane domains of the nicotinic acetylcholine receptor contain alpha-helical and beta structures. *EMBO J.* 13:338–341.
10. Blanton, M. P., and J. B. Cohen. 1994. Identifying the lipid-protein interface of the Torpedo nicotinic acetylcholine receptor: secondary structure implications. *Biochemistry.* 33:2859–2872.
11. Hucho, F., U. Gorne-Tschelnokow, and A. Strecker. 1994. Beta-structure in the membrane-spanning part of the nicotinic acetylcholine receptor (or how helical are transmembrane helices?). *Trends Biochem. Sci.* 19:383–387.
12. Akabas, M. H., and A. Karlin. 1995. Identification of acetylcholine receptor channel-lining residues in the M1 segment of the alpha-subunit. *Biochemistry.* 34:12496–12500.
13. Corbin, J., N. Methot, H. H. Wang, J. E. Baenziger, and M. P. Blanton. 1998. Secondary structure analysis of individual transmembrane segments of the nicotinic acetylcholine receptor by circular dichroism and Fourier transform infrared spectroscopy. *J. Biol. Chem.* 273: 771–777.
14. Kim, J., and M. G. McNamee. 1998. Topological disposition of Cys 222 in the alpha-subunit of nicotinic acetylcholine receptor analyzed by fluorescence-quenching and electron paramagnetic resonance measurements. *Biochemistry.* 37:4680–4686.
15. Barrantes, F. J., S. S. Antollini, M. P. Blanton, and M. Prieto. 2000. Topography of nicotinic acetylcholine receptor membrane-embedded domains. *J. Biol. Chem.* 275:37333–37339.
16. Barrantes, F. J. 2002. Lipid matters: nicotinic acetylcholine receptor-lipid interactions (Review). *Mol. Membr. Biol.* 19:277–284.
17. de Planque, M. R. R., D. T. S. Rijkers, and F. Separovic. 2003. Conformation of the M1 transmembrane segment of the nicotinic acetylcholine receptor in a membrane environment. *Biophys. J.* 84:229A–230A.
18. de Planque, M. R. R., D. T. S. Rijkers, R. M. J. Liskamp, and F. Separovic. 2004. The alpha M1 transmembrane segment of the nicotinic acetylcholine receptor interacts strongly with model membranes. *Magn. Reson. Chem.* 42:148–154.

19. de Planque, M. R., D. T. Rijkers, J. I. Fletcher, R. M. Liskamp, and F. Separovic. 2004. The alphaM1 segment of the nicotinic acetylcholine receptor exhibits conformational flexibility in a membrane environment. *Biochim. Biophys. Acta.* 1665:40–47.

20. Zhang, H., and A. Karlin. 1997. Identification of acetylcholine receptor channel-lining residues in the M1 segment of the beta-subunit. *Biochemistry.* 36:15856–15864.

21. England, P. M., Y. Zhang, D. A. Dougherty, and H. A. Lester. 1999. Backbone mutations in transmembrane domains of a ligand-gated ion channel: implications for the mechanism of gating. *Cell.* 96:89–98.

22. Wang, H. L., A. Auerbach, N. Bren, K. Ohno, A. G. Engel, and S. M. Sine. 1997. Mutation in the M1 domain of the acetylcholine receptor alpha subunit decreases the rate of agonist dissociation. *J. Gen. Physiol.* 109:757–766.

23. Croxen, R., C. Hatton, C. Shelley, M. Brydson, G. Chauplannaz, H. Oosterhuis, A. Vincent, J. Newsom-Davis, D. Colquhoun, and D. Beeson. 2002. Recessive inheritance and variable penetrance of slow-channel congenital myasthenic syndromes. *Neurology.* 59:162–168.

24. Hatton, C. J., C. Shelley, M. Brydson, D. Beeson, and D. Colquhoun. 2003. Properties of the human muscle nicotinic receptor, and of the slow-channel myasthenic syndrome mutant epsilonL221F, inferred from maximum likelihood fits. *J. Physiol.* 547:729–760.

25. Spitzmaul, G., J. Corradi, and C. Bouzat. 2004. Mechanistic contributions of residues in the M1 transmembrane domain of the nicotinic receptor to channel gating. *Mol. Membr. Biol.* 21:39–50.

26. Cordes, F. S., J. N. Bright, and M. S. Sansom. 2002. Proline-induced distortions of transmembrane helices. *J. Mol. Biol.* 323:951–960.

27. Miyazawa, A., Y. Fujiyoshi, and N. Unwin. 2003. Structure and gating mechanism of the acetylcholine receptor pore. *Nature.* 423:949–955.

28. Tang, P., P. K. Mandal, and Y. Xu. 2002. NMR structures of the second transmembrane domain of the human glycine receptor alpha(1) subunit: model of pore architecture and channel gating. *Biophys. J.* 83:252–262.

29. Lobley, A., L. Whitmore, and B. A. Wallace. 2002. DICHROWEB: an interactive website for the analysis of protein secondary structure from circular dichroism spectra. *Bioinformatics.* 18:211–212.

30. Baxter, N. J., and M. P. Williamson. 1997. Temperature dependence of 1H chemical shifts in proteins. *J. Biomol. NMR.* 9:359–369.

31. Wishart, D. S., C. G. Bigam, J. Yao, F. Abildgaard, H. J. Dyson, E. Oldfield, J. L. Markley, and B. D. Sykes. 1995. 1H, 13C and 15N chemical shift referencing in biomolecular NMR. *J. Biomol. NMR.* 6:135–140.

32. Farrow, N. A., R. Muhandiram, A. U. Singer, S. M. Pascal, C. M. Kay, G. Gish, S. E. Shoelson, T. Pawson, J. D. Forman-Kay, and L. E. Kay. 1994. Backbone dynamics of a free and phosphopeptide-complexed Src homology 2 domain studied by 15N NMR relaxation. *Biochemistry.* 33:5984–6003.

33. Delaglio, F., S. Grzesiek, G. W. Vuister, G. Zhu, J. Pfeifer, and A. Bax. 1995. NMRPipe: a multidimensional spectral processing system based on UNIX pipes. *J. Biomol. NMR.* 6:277–293.

34. Goddard, T. D., and D. G. Kneller. 2001. SPARKY 3, University of California, San Francisco, CA.

35. Brünger, A. T. 1992. X-PLOR: a system for x-ray crystallography and NMR, version 3.581, Yale University Press, New Haven, CT.

36. Laskowski, R. A., J. A. Rullmannn, M. W. MacArthur, R. Kaptein, and J. M. Thornton. 1996. AQUA and PROCHECK-NMR: programs for checking the quality of protein structures solved by NMR. *J. Biomol. NMR.* 8:477–486.

37. Cai, M., Y. Huang, R. Zheng, S. Q. Wei, R. Ghirlando, M. S. Lee, R. Craigie, A. M. Gronenborn, and G. M. Clore. 1998. Solution structure of the cellular factor BAF responsible for protecting retroviral DNA from autointegration. *Nat. Struct. Biol.* 5:903–909.

38. Nilges, M., G. M. Clore, and A. M. Gronenborn. 1988. Determination of three-dimensional structures of proteins from interproton distance data by hybrid distance geometry-dynamical simulated annealing calculations. *FEBS Lett.* 229:317–324.

39. Clore, G. M., and A. M. Gronenborn. 1998. New methods of structure refinement for macromolecular structure determination by NMR. *Proc. Natl. Acad. Sci. USA.* 95:5891–5898.

40. Baker, E. N., and R. E. Hubbard. 1984. Hydrogen bonding in globular proteins. *Prog. Biophys. Mol. Biol.* 44:97–179.

41. Mitchell, J. B. O., and S. L. Price. 1990. The nature of the N-H···O:C hydrogen bond: an intermolecular perturbation theory study of the formamide/formaldehyde complex. *J. Comput. Chem.* 11:1217–1233.

42. Koradi, R., M. Billeter, and K. Wuthrich. 1996. MOLMOL: a program for display and analysis of macromolecular structures. *J. Mol. Graph.* 14:51–55, 29–32.

43. Humphrey, W., A. Dalke, and K. Schulten. 1996. VMD: visual molecular dynamics. *J. Mol. Graph.* 14:33–38, 27–38.

44. Kay, L. E. 1998. Protein dynamics from NMR. *Nat. Struct. Biol.* 5(Suppl.):513–517.

45. Lipari, G., and A. Szabo. 1982. Model-free approach to the interpretation of nuclear magnetic resonance relaxation in macromolecules. 2. Analysis of experimental results. *J. Am. Chem. Soc.* 104:4559–4570.

46. Lipari, G., and A. Szabo. 1982. Model-free approach to the interpretation of nuclear magnetic resonance relaxation in macromolecules. 1. Theory and range of validity. *J. Am. Chem. Soc.* 104:4546–4559.

47. Dosset, P., J. C. Hus, M. Blackledge, and D. Marion. 2000. Efficient analysis of macromolecular rotational diffusion from heteronuclear relaxation data. *J. Biomol. NMR.* 16:23–28.

48. Wishart, D. S., B. D. Sykes, and F. M. Richards. 1992. The chemical shift index: a fast and simple method for the assignment of protein secondary structure through NMR spectroscopy. *Biochemistry.* 31: 1647–1651.

49. White, S. H., and W. C. Wimley. 1999. Membrane protein folding and stability: physical principles. *Annu. Rev. Biophys. Biomol. Struct.* 28: 319–365.

50. Kay, L. E., D. A. Torchia, and A. Bax. 1989. Backbone dynamics of proteins as studied by 15N inverse detected heteronuclear NMR spectroscopy: application to staphylococcal nuclease. *Biochemistry.* 28:8972–8979.

51. Brandl, C. J., and C. M. Deber. 1986. Hypothesis about the function of membrane-buried proline residues in transport proteins. *Proc. Natl. Acad. Sci. USA.* 83:917–921.

52. Opella, S. J., F. M. Marassi, J. J. Gesell, A. P. Valente, Y. Kim, M. Oblatt-Montal, and M. Montal. 1999. Structures of the M2 channel-lining segments from nicotinic acetylcholine and NMDA receptors by NMR spectroscopy. *Nat. Struct. Biol.* 6:374–379.

53. Yushmanov, V. E., Y. Xu, and P. Tang. 2003. NMR structure and dynamics of the second transmembrane domain of the neuronal acetylcholine receptor beta 2 subunit. *Biochemistry.* 42:13058–13065.

54. Ma, D., Z. Liu, L. Li, P. Tang, and Y. Xu. 2005. Structure and dynamics of the second and third transmembrane domains of human glycine receptor. *Biochemistry.* 44:8790–8800.

55. Bennett, M., J. A. Yeagle, M. Maciejewski, J. Ocampo, and P. L. Yeagle. 2004. Stability of loops in the structure of lactose permease. *Biochemistry.* 43:12829–12837.

56. Katragadda, M., J. L. Alderfer, and P. L. Yeagle. 2001. Assembly of a polytopic membrane protein structure from the solution structures of overlapping peptide fragments of bacteriorhodopsin. *Biophys. J.* 81: 1029–1036.

57. Card, P. B., and K. H. Gardner. 2005. Identification and optimization of protein domains for NMR studies. *Methods Enzymol.* 394:3–16.

58. Beswick, V., R. Guerois, F. Cordier-Ochsenbein, Y. M. Coic, T. Huynh-Dinh, J. Tostain, J. P. Noel, A. Sanson, and J. M. Neumann. 1998. Dodecylphosphocholine micelles as a membrane like environment: new results from NMR relaxation and paramagnetic relaxation enhancement analysis. *Eur. Biophys. J.* 28:48–58.